Title

CHEMISTRY AND MORPHOLOGY OF COAL LIQUEFACTION QUARTERLY REPORT - JAN. 1 TO MARCH 30, 1981.

Author

Heinemann, H.

Publication Date

1981-03-01

LBL-12933
UC-90d

Lawrence Berkeley Laboratory
UNIVERSITY OF CALIFORNIA

Materials & Molecular Research Division

CHEMISTRY AND MORPHOLOGY OF COAL LIQUEFACTION
QUARTERLY REPORT - January 1 to March 30, 1981

Heinz Heinemann

March 1981

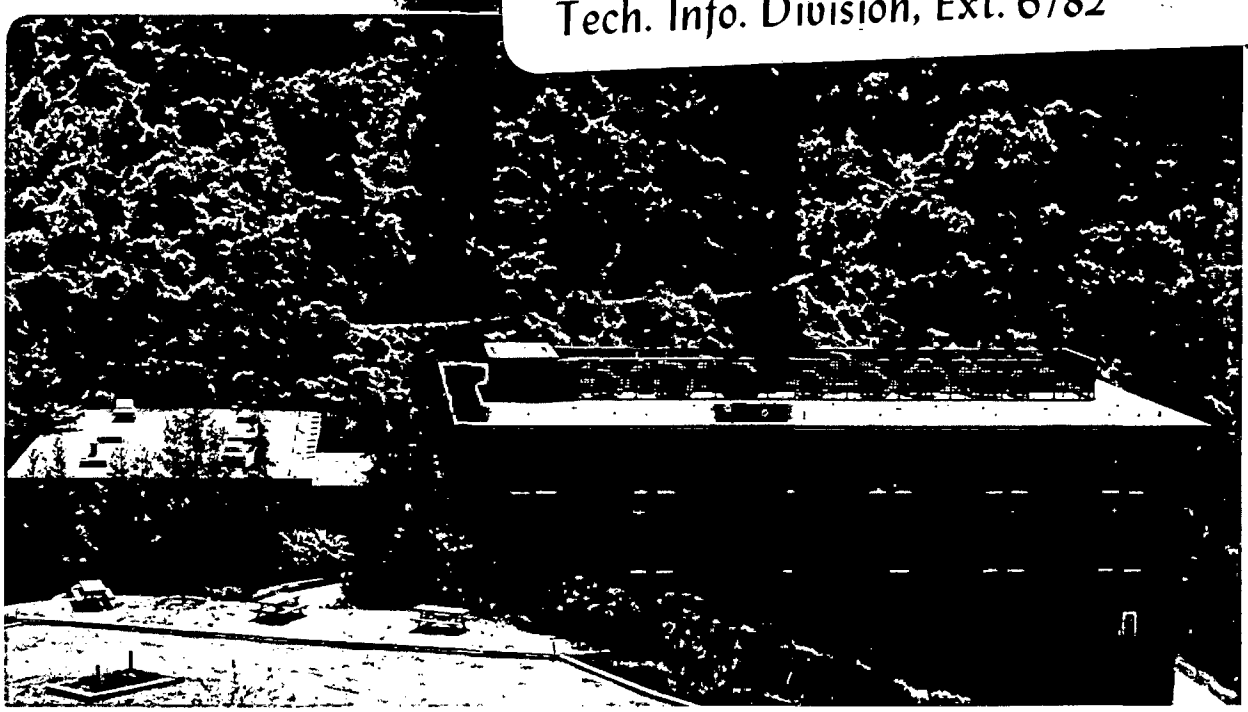

Prepared for the U.S. Department of Energy under Contract W-7405-ENG-48

DISCLAIMER

LBL-12933

QUARTERLY REPORT

January 1 to March 30, 1981

CHEMISTRY AND MORPHOLOGY OF COAL LIQUEFACTION

Contract No. 3425

Principal Investigator: Heinz Heinemann

Lawrence Berkeley Laboratory

University of California

Berkeley, CA 94720

This work was jointly supported by the Director, Office of Energy Research, Office of Basic Energy Sciences, Chemical Sciences Division and the Assistant Secretary for Fossil Energy, Office of Coal Research, Liquefaction Division of the U.S. Department of Energy under Contract W-7405-ENG-48 through the Pittsburgh Energy Technology Center, Pittsburgh, PA.

Contents

		Page
I	Cover Sheet	1
II	Technical Program for Fiscal 1981	2
III	Highlights	4
IV	Progress of Studies	
	Task 1	5
	Task 2	6
	Task 3	6
	Task 4	9
	Task 5	9
	Task 6	13

II Technical Program for Fiscal 1981

TASK 1 - Selective Synthesis of Gasoline Range Components from Synthesis Gas - A. T. Bell

Preparation of a series of iron catalysts supported on Al_2O_3 and promoted with potassium in different ratios. Surface and compositional analysis of the catalysts and testing of them for the conversion of $CO+H_2$ in a slurry reactor. Investigation of the effect of shape selective catalyst components on product distribution. Investigation of transport phenomena of CO and H_2 through a liquid film on the catalyst.

TASK 2 - Electron Microscope Studies of Coal During Hydrogenation J. W. Evans

Reaction of single crystal graphite with predetermined gas mixtures in the environmental cell of a 650 Kv electron microscope. Morphological changes of the graphite at different temperatures and pressures will be observed while chemical products will be identified in a masspectrometer attached to the cell. Reactions will be studied in the presence and absence of catalysts and will be extended to coals of high crystalline character.

TASK 3 - Catalyzed Low Temperature Hydrogenation of Coal - G. A. Somorjai

Transition metal catalysts will be deposited on a coal surface. Hydrogenation or steam-carbon reactions will be carried out on these samples at low temperatures (150-400°C). Catalyst-coal surface changes will be observed at various stages of reaction by means of a low pressure-high pressure apparatus, permitting the analysis of the surface structure and surface composition of reactants and catalysts. Surface science techniques such as Auger and photo electron spectroscopy will be applied.

TASK 4 - Selective Hydrogenation, Hydrogenolysis and Alkylation of Coal and Coal Liquids by Organo Metallic Systems K. P. C. Vollhardt

Study of novel transition metal catalysts, capable of cleavage of carbon-carbon and carbon-heteroatom bonds with concomitant reduction. Application of findings to selective coal depolymerization, hydrogenation and liquefaction under mild conditions.

TASK 5 - Chemistry of Coal Solubilization and Liquefaction R. G. Bergman

This study will concentrate on the hydrogen transfer from donor molecules such as tetralin to condensed aromatic coal-like molecules. Both thermal and catalytic mechanisms will be investigated with the ultimate objective of a catalytic donor mechanism at lower temperatures than are used in current practice.

TASK 6 - Coal Conversion Catalysts-Deactivation Studies
A. V. Levy and E. E. Petersen

Cobalt-molybdena-alumina catalysts will be aged by metal deposition under controlled conditions and a mechanism for scale formation on spent catalysts will be defined. Porosity and diffusion measurements will determine whether the scales form a diffusion barrier.

III Highlights

1. All tasks of the program were active during the report quarter, and are discussed in Section IV. A presentation of work accomplishments was made to DOE, BES Chemical Sciences, and DOE Fossil Energy personnel on March 3, 1981.

2. Ash from a high volatile bituminous coal was studied in the electron microscope to determine whether the ash or the original coal contain identifiable titanium minerals. While titanium is detectable in certain ash particles, no ash particle was found that consists mainly of a titanium mineral.

3. In the course of observing by means of Auger spectroscopy graphite gasification reactions catalyzed by metals, it has been found that in the presence of hydrogen, nickel appears to diffuse from the surface into the bulk of the graphite. When potassium is deposited on graphite, it is volatilized above 400°C. Surprisingly the production of methane and carbondioxide from the reaction of graphite and steam was catalyzed by potassium at as low a temperature as 250°C.

4. It has been shown that literature on the alkylation of benzene with synthesis gas is erroneous and that the products reported are due to Lewis acid catalyzed cracking of benzene. A novel cobalt mediated, reversible cleavage of a vinyl-hydrogen bond has been discovered.

5. All products from the thermal decomposition of tetralin have been identified. The stereochemistry of cis-1, 2 dihydrotetralin was determined.

6. In the utilization of the water gas shift reaction as a reducing agent for model coal compounds it has been found that tributylphosphine ligands increase the life of transition metal hydride catalysts.

7. Rates of demetallation of high metal content gas oils over cobalt-molybdena-alumina catalysts were measured for vanadium and iron. Kinetic analysis is under way. It is clearly shown that pore plugging of the catalyst occurs early and results in deposition of the metals on the external catalyst surface.

IV Progress of Studies

TASK 1 - Selective Synthesis of Gasoline Range Components from Synthesis Gas. Task Manager: A. T. Bell

Proper operation of the fixed bed reactor was established using a synthetic ammonia iron catalyst. Since this catalyst is not exceptionally active for Fischer-Tropsch synthesis, it was replaced by a precipitated iron catalyst, promoted with copper and potassium. Tests of this catalyst show that on a gram basis it is more active than the synthetic ammonia catalyst and appears to be somewhat more stable. During the past six weeks, several attempts have been made to explore the dependence of conversion and product selectivity on reactant space velocity, using this catalyst. In each case, the run had to be terminated before completion due either to decay in catalyst activity with time or plugging of the transfer line from the reactor with wax. The latter problem has been traced to the burnout of the heater used to maintain the transfer line at elevated temperature. Replacement of the heater and insertion of a larger diameter transfer line is expected to eliminate this problem.

Since the catalyst activity gradually declines by about 50 to 70% over several days of operation at a fixed set of conditions, it is difficult to establish the extent to which changes in product composition observed upon changing space velocity are due to change in this variable or to catalyst deactivation. Because of the very long time required to achieve steady-state (1-2 days) at each set of operating conditions, the conduct of runs requiring a week or more of steady operation is becoming impractical. As a result, strategies for accelerating the data acquisition process are now being evaluated.

The autoclave reactor has also been put into operation during the past quarter. Problems were encountered initially with overheating of the stirrer bearing. This situation has been eliminated by placement of a cooling jacket just above the bearing. Preliminary runs made with this reactor have been successful in producing products and have shown that very little of the paraffin wax, used as the suspending medium for the catalyst, is lost from the reactor. At present, studies are being conducted to establish the extent to which the paraffin wax undergoes hydrogenolysis. Analysis of the off gas produced during catalyst reduction has shown a considerable amount of C_5-C_{18} material. As yet it is not clear whether these products are impurities in the wax, which is mainly C_{25} paraffins, or are produced by hydrogenolysis of the wax. The origin of the products needs to be established in order to assess the extent to which they contribute to the product spectrum observed under synthesis conditions.

TASK 2 - Electron Microscope Studies of Coal During Hydrogenation
Task Manager: J. W. Evans

The characterization of coals and mineral matter therein is one aspect of this investigation. The attached Figure 1 illustrates typical results obtained on LBL's analytical electron microscope. The sample represents ash from a high volatile bituminous coal supplied by Dr. Sid Pollack of the Pittsburgh Energy Technology Center; interest here is in determining whether the ash and original coal contains identifiable titanium minerals. The micrograph shows several ash particles mounted on a carbon film supported by a copper grid. The figures obtained by energy dispersive analysis of X-rays emitted from the sample correspond to the number particles in the micrograph; thus LTA PSOC 1082/1 corresponds to the particle numbered one in the micrograph, and can be tentatively identified as a calcium silicate with a small amount of associated iron sulfide. The strong copper peaks arise from the copper support. Particles 2 and 5 appear to be aluminum silicates, while particle 7 also yields a strong calcium peak. Particles 3, 4, and 6 appear to be iron sulfides. While titanium is detectable in particles 2, 4, and 5, we have yet to discover an ash particle that is mainly a titanium mineral.

In a related part of this investigation, an environmental cell (within a high voltage electron microscope) and a mass spectrometer are to be used to observe pyrolysis and carbon reactions with gases and identify reaction products. While the environmental cell has not been used this quarter due to a malfunctioning heater, the mass spectrometer has been tested on known gas mixtures and detects gas components which may be expected from reactions to be studied.

TASK 3 - Catalyzed Low Temperature Hydrogenation of Coal
Task Manager: G. A. Somorjai

1. Graphite and Nickel

A piece of pyrolytic graphite with some nickel deposited onto its surface was hydrogenated at 745°C, as mentioned in the last report. The product of gasification was methane; after a few minutes the reaction stopped. In order to understand this poisoning effect, the time-dependent concentration of nickel on the surface of the graphite was studied by means of Auger spectroscopy in high vacuum. It was observed that nickel was disappearing from the graphite surface when it was heated at elevated temperatures. This change in nickel concentration at the surface starts to be significant at 560°C. At 800°C after 30 seconds, no nickel could be detected on the surface by means of Auger spectroscopy. From the rate of nickel disappearance measured at different temperatures, an activation energy of 22 ± 3 Kcal/mole was estimated. These experiments were done while the mass spectrometer was tuned at mass 59 (nickel) and no evaporated nickel was ever detected.

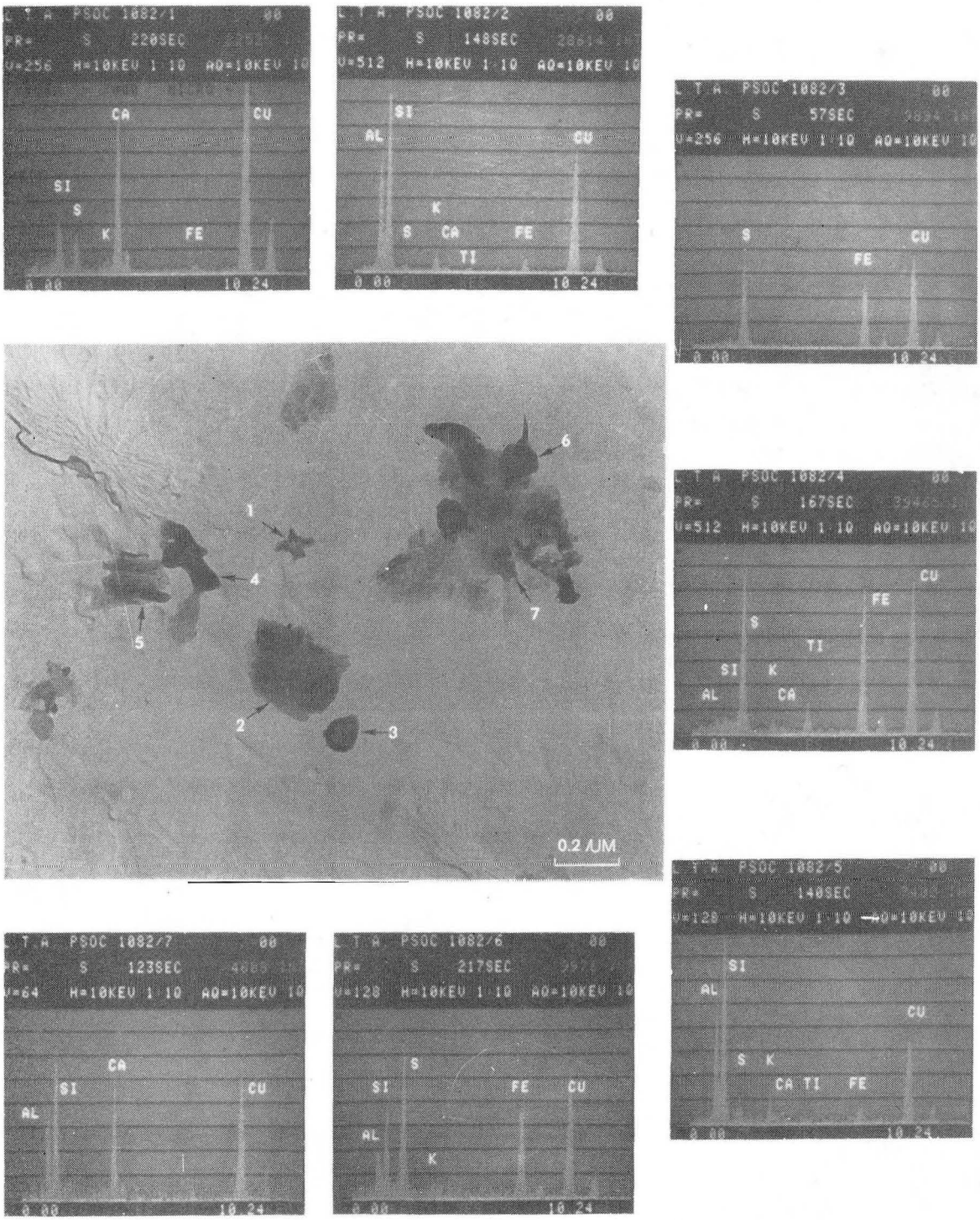

Fig. 1

XBB813-2549

A tentative explanation of the results obtained in these experiments is: Nickel helps to dissociate hydrogen. The atomic hydrogen is very reactive and readily combines with carbon to form methane. On the other hand, nickel diffuses into the bulk of the graphite and when all the nickel has disappeared from the surface the reaction stops.

2. Graphite and Potassium

The aim of our studies of graphite gasifiction is to find a catalyst for gasification at low temperatures. It is well known that potassium carbonate is being used to produce hydrocarbons from steam and coal at relatively low temperatures. Therefore, a study of the interaction of potassium and graphite in different gas atmospheres was initiated. Multilayers of potassium were deposited on graphite using a potassium-zeolite gun at a background pressure of 1×10^{-9} torr. Potassium is quite volatile and some change may occur in the potassium concentration when the graphite is being heated. The potassium-graphite system was therefore studied at different temperatures prior to investigating the interaction of this system with gases. In fact, when the sample is flashed to 800°C, the potassium is completely desorbed from the surface with the maximum of the desorption peak laying at 470°C. The desorption of the potassium is much more severe at ultra high vacuum conditions and is somewhat depressed at high pressures even in a helium atmosphere. At temperatures below 400°C, some potassium stays on the surface. The graphite with potassium was then exposed to different gases in the temperature range of 200-400°C to study the following gasification reactions:

1) $O_2 + C \rightarrow CO_2$

2) $2H_2 + C \rightarrow CH_4$

3) $CO_2 + C \rightarrow CO$

4) $H_2O + C \rightarrow CO + H_2$

5) $2\ H_2O + 2C \rightarrow CH_4 + CO_2$

The first three reactions were not observed even where the gas pressure was as high as 5 atmospheres.

Reactions 4 and 5 were studied with water vapor (32 torr) in helium with a total pressure of 1 atm. Reaction 4 was successful and surprisingly at these low temperatures some methane (equation 5) was also being produced. The concentrations of methane and carbon dioxide were monitored and they were consistently increasing in a period of at least two hours. The maximum conversion to methane occurred at 250°C and was $3.5\ 10^{-5}$. From the rates measured at different temperatures, an activation energy of 5.6 Kcal/mole was estimated.

We are presently involved in finding out the nature of the potassium on the graphite surface as well as some loss of the potassium even at low temperatures. We suspect that the potassium is diffusing into the bulk of the graphite at low temperatures similar to the case of nickel. This loss of potassium at low temperatures can be expected to eventually terminate the reaction.

TASK 4 - Selective Hydrogenation, Hydrogenolysis and Alkylation of Coal and Coal Liquids by Organo Metallic Systems
Task Manager: K. P. C. Vollhardt

1. Friedel-Crafts Alkylation and Cleavage of Benzene

The purported Fischer-Tropsch alkylation of benzene with $W(CO)_6$-$AlCl_3$ is shown to be a result of the Lewis acid catalyzed cracking of benzene. Thus, ^{13}CO or D_2 are not incorporated in the alkylbenzene products, nor are they necessary for their formation. The reaction proceeds in the absence of the transition metal "catalyst." A 1:1 mixture of benzene and benzene-^{13}C furnishes the appropriately labeled cracking and condensation products with varying degrees of ^{13}C-scrambling. See Table 1, Figures 2 and 3.

2. Models for Metal Catalyzed Thermal Hydrogen Shifts

We have uncovered a novel cobalt-mediated rearrangement of a η^6- 1,3,5-hexatriene ligand in which a vinyl-hydrogen bond is cleaved reversibly. This constitutes a very unusual and exceedingly facile C_{sp_2}-H activation step. Such processes will have to be considered as being contributors to hydrogen shifts in coal pyrolysis reactions. X-ray structures are being determined and mechanistic details investigated by labelling and kinetic experiments.

TASK 5 - Chemistry of Coal Solubilization and Liquefaction Pyrolysis Studies
Task Managers: R. G. Bergman, T. Vermeulen and R. H. Fish

1. Mechanism of Dehydrogenation of Tetralin

All six major products from the thermal decomposition of tetralin have been isolated and conclusively identified. These products were styrene, benzocyclobutene, indene, o-allyltoluene, 1,2-dihydronaphthalene, and naphthalene. Isolation was accomplished by preparative gas chromatography on a 15' x 3/8" 20% OV-17 column. Identification was accomplished by comparison of both infrared (IR) and nuclear magnetic resonance (NMR) spectra with those of authentic samples. Authentic samples of benzocyclobutene and o-allyltoluene were prepared by independent synthetic routes. All other samples were commercially available.

The stereochemistry of cis-1, 2-dihydrotetralin-d_{10} was unambiguously determined by 2-dimensional (2D) NMR spectroscopy. This technique

TABLE 1 Product yields from the $AlCl_3$/benzene reaction under various conditions.

Conditions:	$[AlCl_3]$ = 0.7M N_2 (1 atm), 160°, 48h	$[AlCl_3]$ = 0.25M N_2 (120 atm), 200°, 3h	$[AlCl_3]$ = 0.25M, 200°, 3h $[W(CO)_6$/diphos][b], H_2(100 atm)/CO (20 atm)
% Yield[a] of:			
Toluene	2.187	1.153	1.076, (0.973)[c], (1.134)[d]
Ethylbenzene	2.680	1.336	1.660, (1.745)[c], (2.074)[d]
i-Propylbenzene	0.182	0.048	0.174, (0.044)[c], (0.137)[d]
n-Propylbenzene	0.331	0.090	Trace, (0.069)[c], (0.012)[d]
Butylbenzenes	0.110	0.011	Trace, (0.021)[c], (0.044)[d]
Tetralin	0.726	0.019	0.037, (0.035)[c], (0.050)[d]
Phenylcyclohexane	0.059	0.007	0.019, (0.009)[c], (0.034)[d]
Biphenyl	1.548	0.081	0.036, (0.129)[c], (0.159)[d]
Diphenylmethane	0.228	0.021	5.973, (0.151)[c], (0.562)[d]
Diphenylethane(s)	0.340	0.024	0.146, (0.064)[c], (0.280)[d]

[a] GC yield calculated using n-octane as internal standard. These products were characterized by GC/MS and co-injection of authentic samples.

[b] $[W(CO)_6]$ = [diphos] = 0.0047M

[c] Yield from reaction in the absence of $W(CO)_6$

[d] Yield from reaction in the absence of diphos.

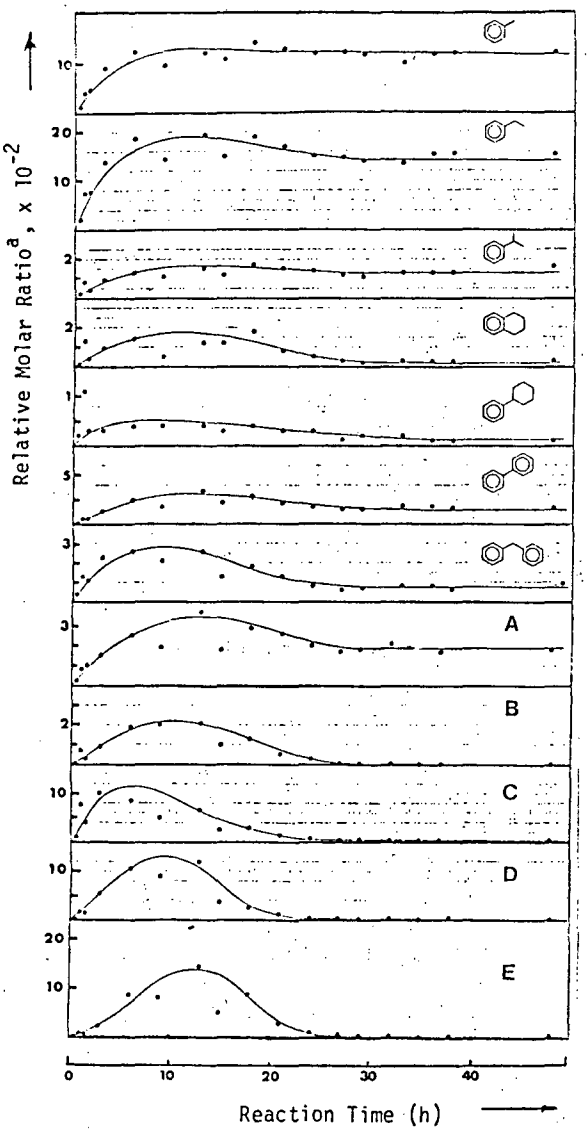

FIGURE 2. Plot of relative molar ratio[a] versus reaction time in the $AlCl_3$/Benzene reaction ([$AlCl_3$] = 0.7M, N_2 (1 atm), 160°, 48h).

A: 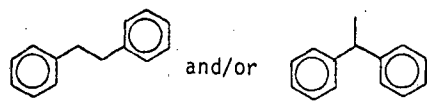 and/or

B: 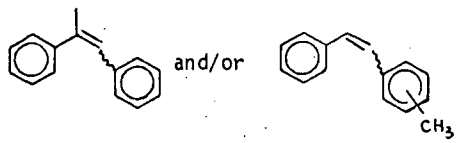

C,D: 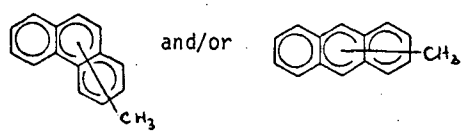

E: 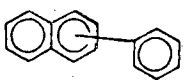

[a] n-Octane was used as internal standard.
Different scales have been used for clarity.

FIGURE 3 A typical GC of the products from the reaction of benzene and $AlCl_3$ ($[AlCl_3]$ = 0.7M, N_2 (1 atm), 160°, 48h).

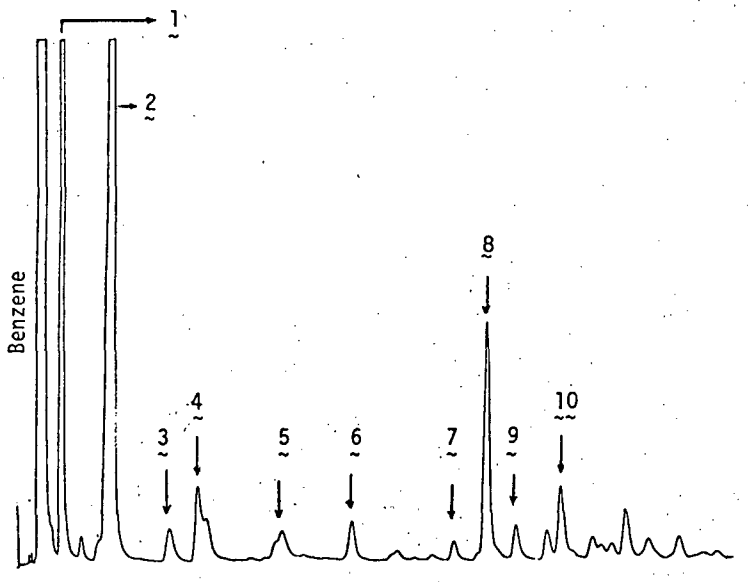

Major products identified by co-injection of authentic samples and GC/MS:

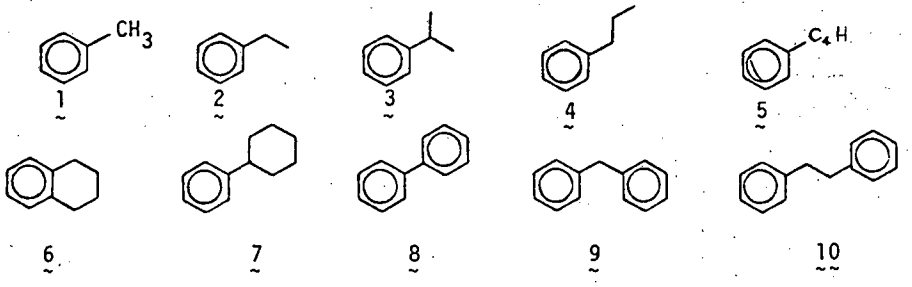

1 2 3 4 5 6 7 8 9 10

Minor products identified by GC/MS:

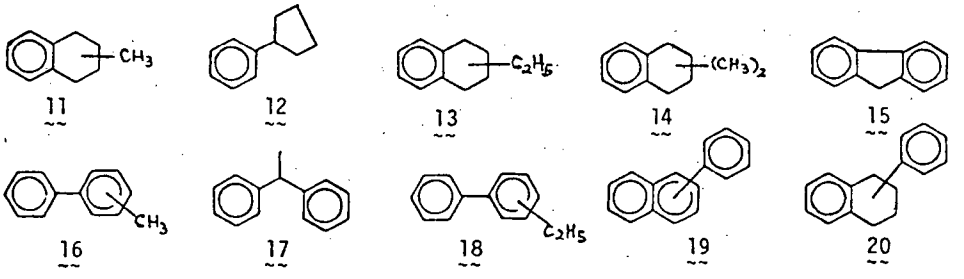

11 12 13 14 15 16 17 18 19 20

utilized a spin-echo pulse sequence which results in suppression of the heteronuclear couplings since the spin states of the heteronuclear couplings since the spin states of the heteronuclei are not directly affected by the 180° pulse. A 90° projection of a 2D J spectrum of 1,2=dihydrotetralin-d_{10} displays the proton-proton coupling constant, which in principle allows the determination of the realtive orientation of the two protons. A ± 14.7 Hz sweep width in the f_1 dimension with a frequency resolution of 0.12 Hz results in a coupling constant of 5.5 Hz, consistent with a cis-stereochemistry.

2. Hydrogen Transfer Mechanism Studies

In continuing to define the utility of carbon monoxide and water, as a reducing agent for model coal constituents, we have attempted to ascertain the parameters needed to stabilize the catalytically generated transition metal hydrides.

We have found that the reduction reaction with anthracene is limited by temperature as related to intermediate hydride stability. In order to increase transition-metal hydride lifetimes, we have added stabilizing ligands and studied the effects of increasing the partial pressure of carbon monoxide as well as adding hydrogen gas.

We find that tributylphosphine ligands do indeed increase transition metal hydride lifetimes and thereby increase the amount of 9,10-dihydroanthracene produced in the reduction reaction (Table 2). However, neither increasing the partial pressure of carbon monoxide nor adding hydrogen gas seems to affect the amount of reduction product observed.

We will continue to peruse the transition metal carbonyls that produce the more stable transition metal hydrides and further our knowledge of the reactivity of other model coal compounds such as pyrene quinoline, benzophenone, benzyl ethers and substituted phenanthrene derivatives.

TASK 6 - Coal Conversion Catalysts - Deactivation Studies
Task Managers: A. V. Levy and E. E. Petersen

Hydrodemetallation studies of gas oil enriched with metallic naphthenates were carried out using the semi-continuous high pressure reactor system described in previous reports. Eighteen catalyst-aging runs were performed at varying reaction conditions using a commercial hydrotreating catalyst (American Cyanamid Trilobe HDS-20). During the runs, liquid product samples were collected at regular intervals, and analyzed for metals using X-ray fluorescence spectrometry. The fresh and aged catalysts were evaluated by optical and scanning electron microscopes equipped with the KEVEX facility. Surface areas of fresh and aged catalysts were measured by BET apparatus.

Table 2

Catalyst	Substrate	S/C	Temp (°C)	Time (hr)	Base	CO (psi)	Products
$Fe(CO)_5$	anthracene	20	160	24	Me_3N/H_2O	350	0.5% 9,10-dihydroanthracene; WGS
$Fe(CO)_5$	"	10	150	20	0.2M KOH	350	6% 9,10-dihydroanthracene
$Fe(CO)_4Bu_3P$	"	10	200	2	"	"	7% 9,10-dihydroanthracene
				24			11% 9,10-dihydroanthracene
$Fe(CO)_4Bu_3P$	"	10	200	2	0.1M $KHCO_3$	350 + 350 psi H_2	7% 9,10-dihydroanthracene
$Mn_2(CO)_{10}$	"	20	150	5	0.1M $KHCO_3$	350	1% 9,10-dihydroanthracene
$Mn_2(CO)_{10}$	"	20	160	5	D_2O	350	5% 9,10-dideuteroanthracene
$Mn_2(CO)_{10}$	"	20	160	5	$(Me)_3N/H_2O$	350	—
$Mn_2(CO)_{10}$	phenanthrene	20	160	10	H_2O	350	—
$Mn_2(CO)_{10}$	anthracene	20	180	5	H_2O	350	7% 9,10-dihydroanthracene
$Mn_2(CO)_{10}$	"	20	180	5	H_2O	500	6% 9,10-dihydroanthracene
$Mn_2(CO)_{10}$	"	20	180	5	0.2M KOH	350	6% 9,10-dihydroanthracene
				24			9% 9,10-dihydroanthracene
$Mn_2(CO)_9Bu_3P$	"	20	180	5	0.2M KOH	350	5% 9,10-dihydroanthracene
				20			12% 9,10-dihydroanthracene
$Mn_2(CO)_8(Bu_3P)_2$	"	20	180	5	0.2M KOH	350	13% 9,10-dihydroanthracene
				20			22% 9,10-dihydroanthracene
$Mn_2(CO)_8(Bu_3P)_2$	"	20	180	5	0.2M KOH	350 + 350 psi H_2	17% 9,10-dihydroanthracene
				20			26% 9,10-dihydroanthracene

TABLE 2, CONTINUED

$Mn_2(CO)_8(Bu_3P)_2$	anthracene	20	200	5	0.2M KOH	350	13% 9,10-dihydroanthracene
				24			13% 9,10-dihydroanthracene
$Ru_3(CO)_{12}$	"	100	100,160	10,10	Me_3N/H_2O	350	excellent WGS
$Ru_3(CO)_{12}$	"	30	160	10	H_2O	350	WGS
$Rh_6(CO)_{16}$	"	60	120,160	5,5	0.1M $KHCO_3$	350	WGS
$Mo(CO)_6$	"	10	160	12	H_2O	350	1% 9,10-dihydroanthracene
$Mo(CO)_5Bu_3P$	"	10	200	20	0.2M KOH	350	2% 9,10-dihydroanthracene
							WGS
$[Co(CO)_3(C_6H_5)P]_2$	"	20	160	5	0.2M KOH	350	2.5% 9,10-dihydroanthracene

The results of two typical runs conducted at different temperatures but at the same pressure, and at relatively high metal concentrations are shown in Figures 3 and 4, wherein the concentrations of vanadium and iron in the product were plotted as a function of time. As shown in Figure 4, the rate of reaction at 300°C was rather slow. Consequently, most of the runs were conducted at 350°C. The demetallation rate at high metal concentrations was observed to be nearly second order but decreased to about half order at metal concentrations below 50-60 ppmw. A detailed analysis of kinetic results of demetallatiln reaction is under way.

The measured distribution of metals near the edge is plotted in Figure 5. The build-up of vanadium concentration over the surface of two catalyst samples of different ages is shown in Figure 6. It appears that the deposited metal in the pores of the catalyst makes further diffusion of metals increasingly difficult. This leads to further deposition of the metal near the edge. The surface area of a catalyst aged for 60h was 93 m^2/g while that of the fresh catalyst was 212 m^2/g.

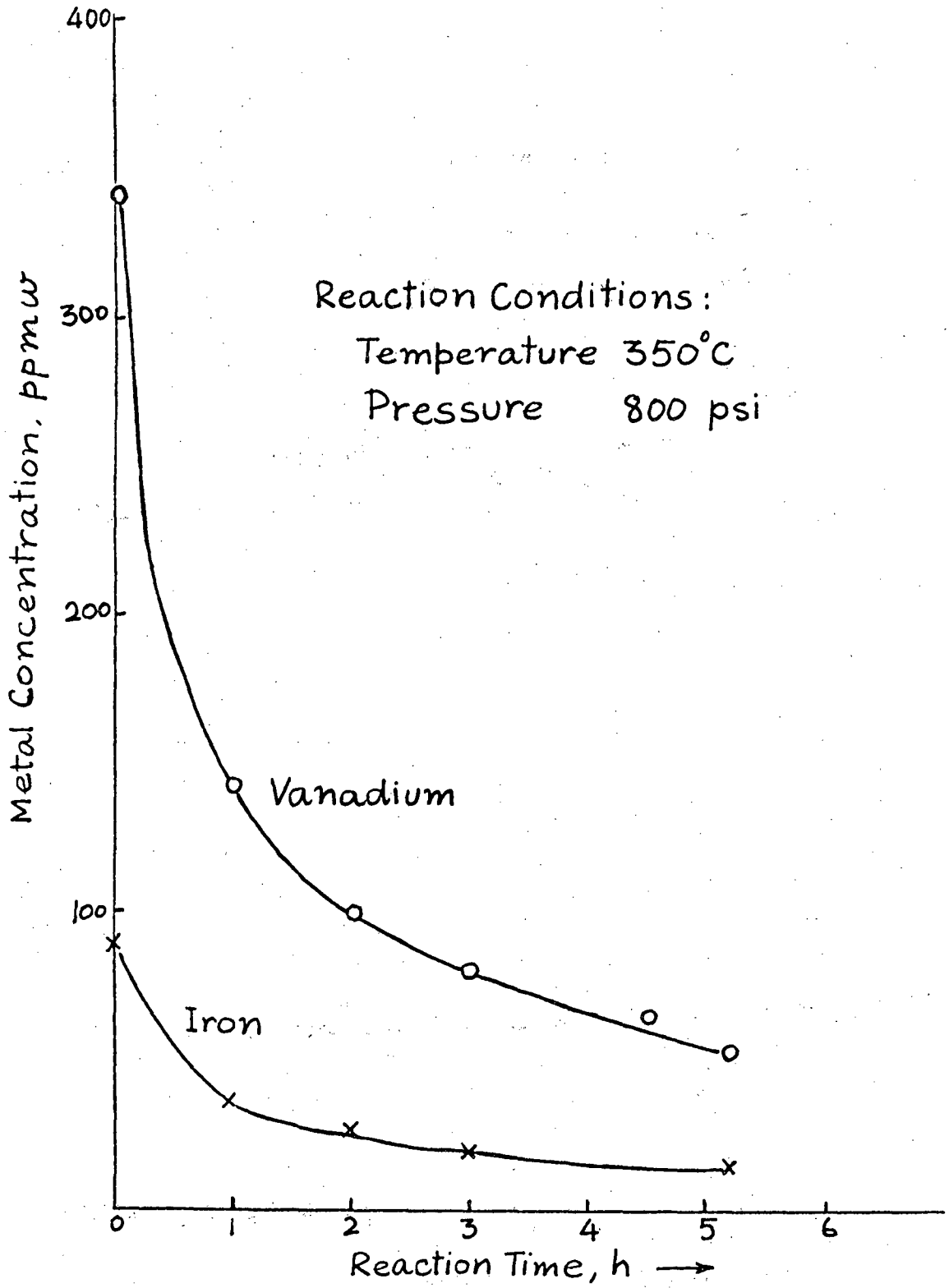

Fig. 3 Metal concentration in the product as a function of time

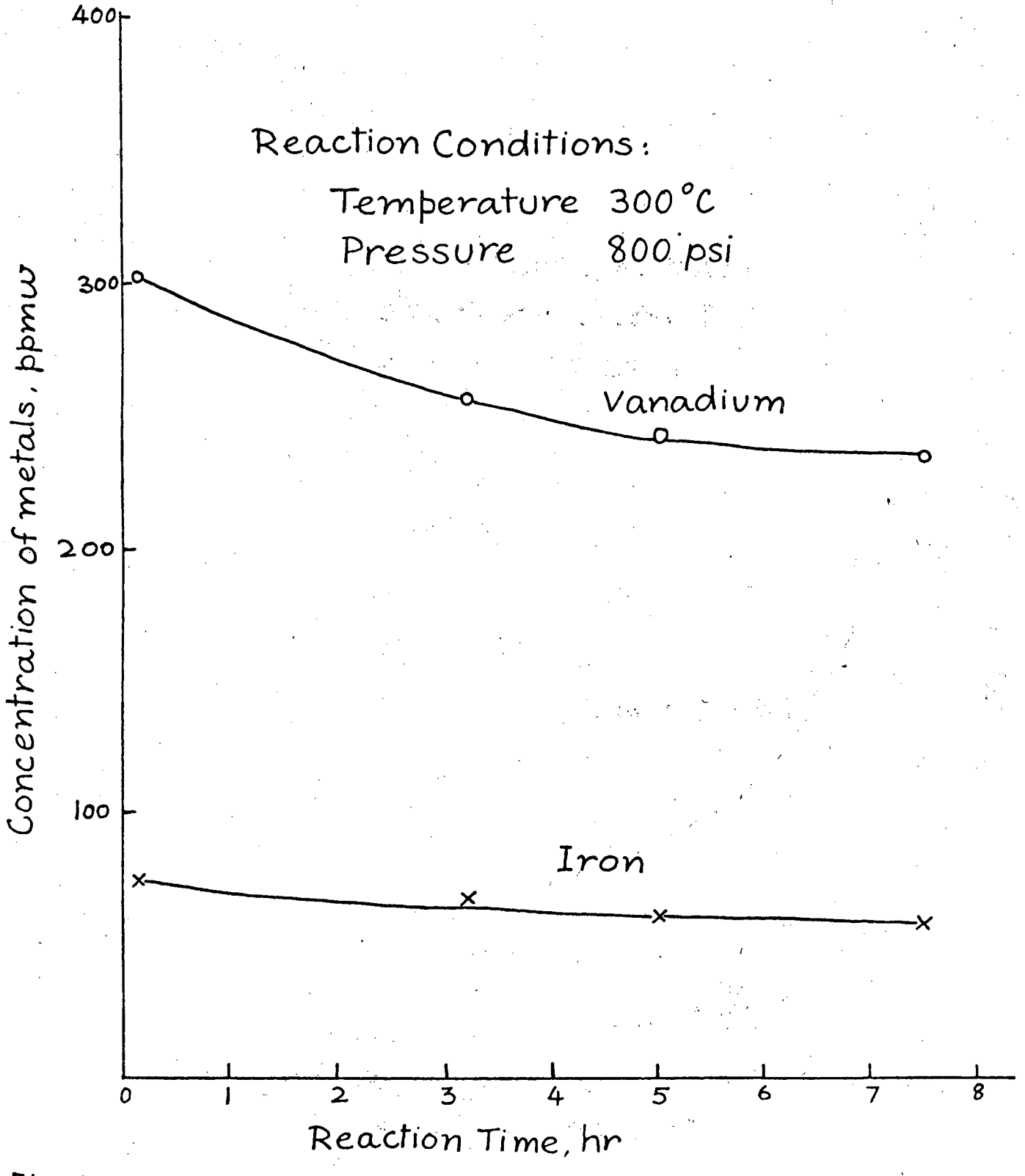

Fig. 4 Metal concentration in the product as a function of time

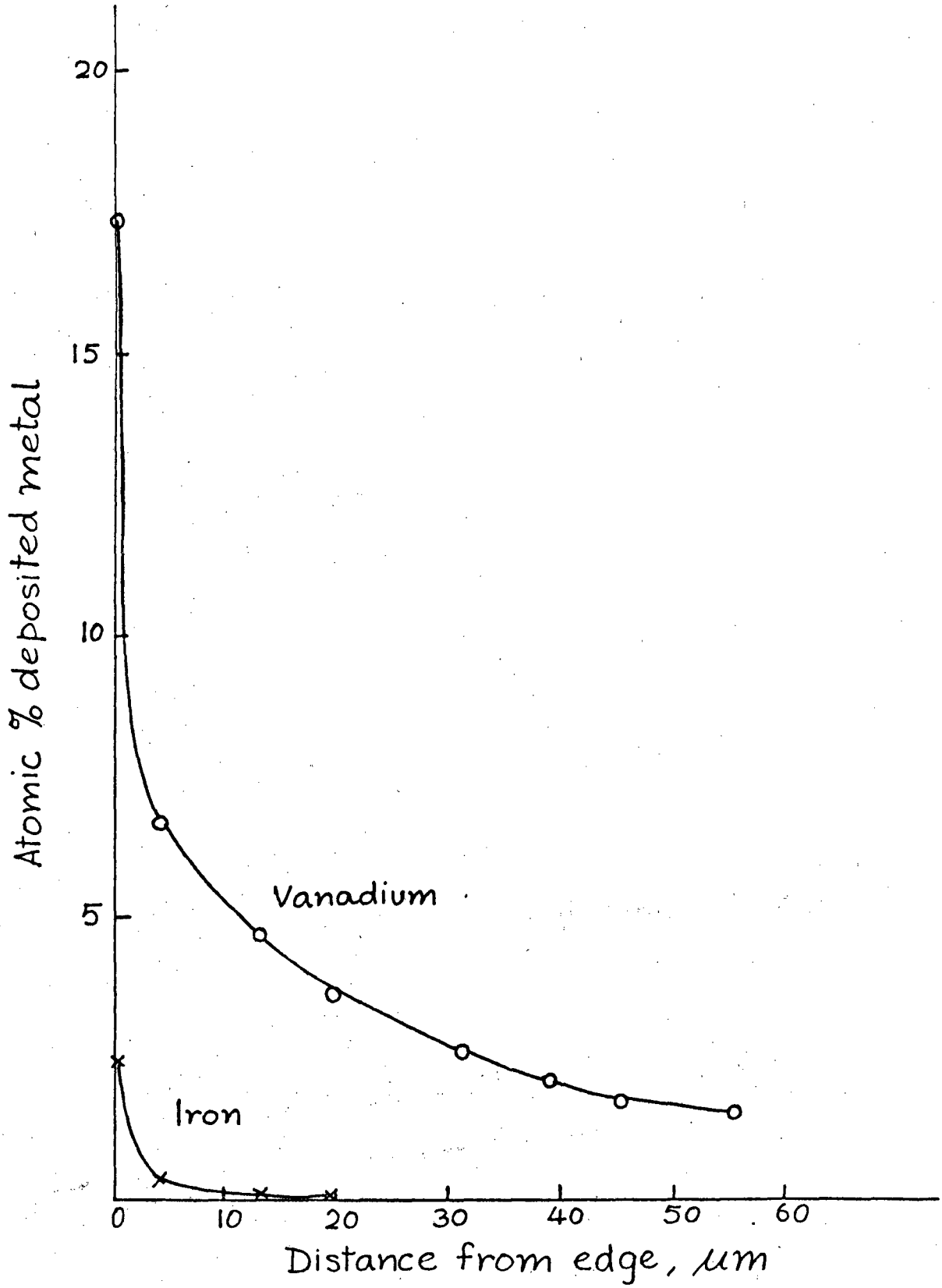

Fig. 5 - Typical distribution of vanadium and iron deposition on the catalyst of 60 h of age

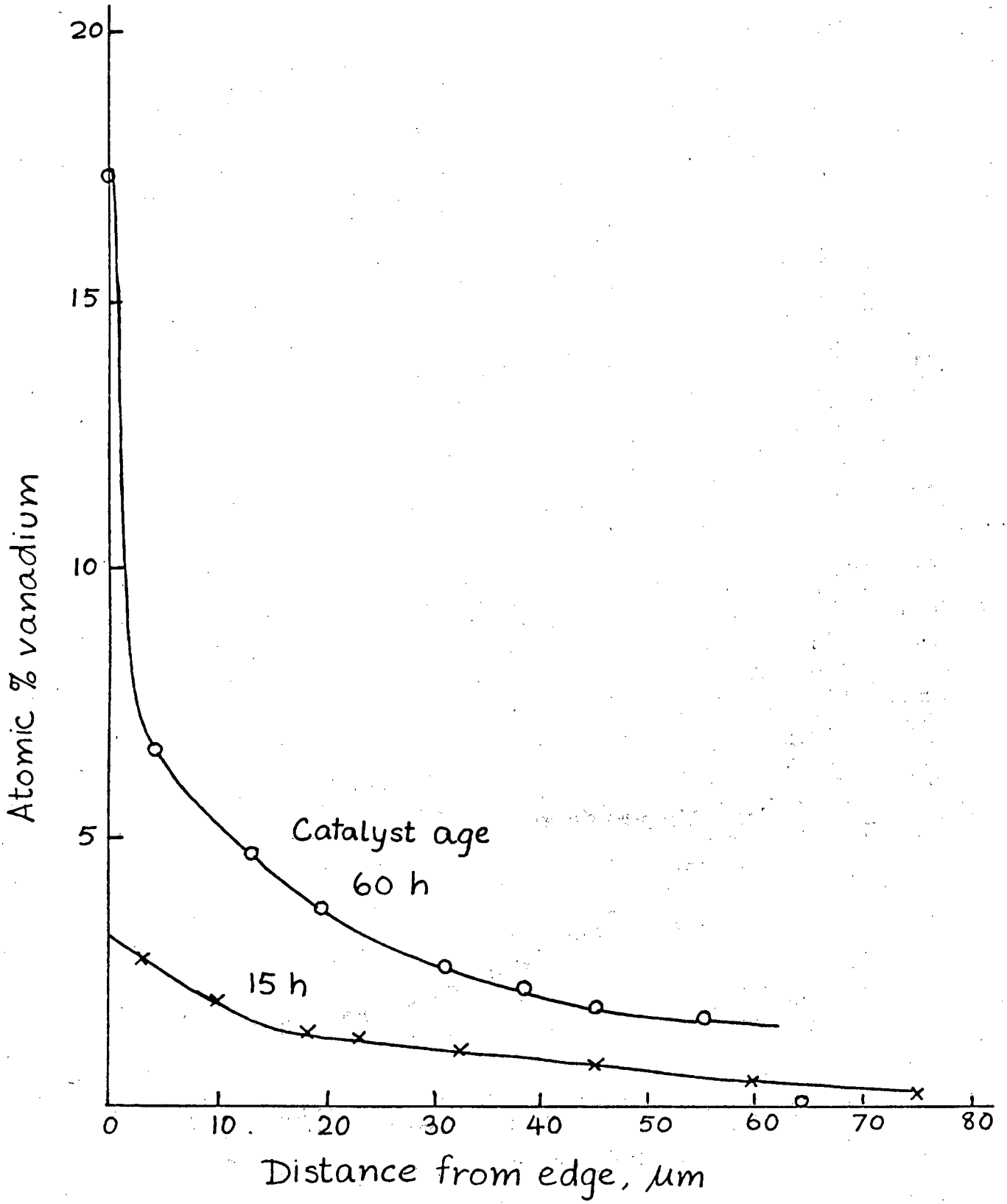

Fig. 6 - Vanadium distribution as a function of distance

TECHNICAL INFORMATION DEPARTMENT
LAWRENCE BERKELEY LABORATORY
UNIVERSITY OF CALIFORNIA
BERKELEY, CALIFORNIA 94720